Growth Differentiation Factor-15–Induced Contractile Activity and Extracellular Matrix Production in Human Trabecular Meshwork Cells

Arumugam Ramachandran Muralidharan,[1] Rupalatha Maddala,[1] Nikolai P. Skiba,[1] and Ponugoti Vasantha Rao[1,2]

[1]Department of Ophthalmology, Duke University School of Medicine, Durham, North Carolina, United States
[2]Department of Pharmacology and Cancer Biology, Duke University School of Medicine, Durham, North Carolina, United States

Correspondence: Ponugoti Vasantha Rao, Duke Eye Center, 2351 Erwin Road, Durham, NC 27710, USA; p.rao@dm.duke.edu.

Submitted: September 2, 2016
Accepted: October 26, 2016

Citation: Muralidharan AR, Maddala R, Skiba NP, Rao PR. Growth differentiation factor-15–induced contractile activity and extracellular matrix production in human trabecular meshwork cells. *Invest Ophthalmol Vis Sci*. 2016;57:6482–6495. DOI: 10.1167/iovs.16-20671

Purpose. To determine the role and regulation of growth differentiation factor-15 (GDF-15), a TGF-β–related cytokine in human trabecular meshwork (TM) cells in the context of aqueous humor (AH) outflow and IOP.

Methods. Regulation of expression by external cues, and the distribution and secretion of GDF-15 by human TM primary cell cultures, and the effects of recombinant (r) GDF-15 on TM cell contractile characteristics, actin cytoskeleton, cell adhesion, extracellular matrix (ECM), α-smooth muscle actin (αSMA), SMAD signaling, and gene expression were determined by immunoblot, immunofluorescence, mass spectrometry, cDNA microarray, and real-time quantitative PCR (RT-qPCR) analyses.

Results. Growth differentiation factor-15, a common constituent of ECM derived from the human TM cells, was confirmed to be distributed throughout the conventional aqueous humor outflow pathway of the human eye. Growth differentiation factor-15 protein levels were significantly increased in human TM cells in response to TGF-β2, dexamethasone, endothelin-1, lysophosphatidic acid, TNF-α, IL-1β treatment, and by cyclic mechanical stretch. Stimulation of human TM cells with rGDF-15 caused a significant increase in the formation of actin stress fibers and focal adhesions, myosin light chain phosphorylation, SMAD signaling, gene expression, and the levels of αSMA and ECM proteins.

Conclusions. The results of this study, including a robust induction of GDF-15 expression by several external factors known to elevate IOP, and rGDF-15–induced increase in contractility, cell adhesion, and the levels of ECM proteins and αSMA in TM cells, collectively suggest a potential role for GDF-15 in homeostasis and dysregulation of AH outflow and IOP in normal and glaucomatous eyes, respectively.

Keywords: trabecular meshwork, GDF-15, glaucoma

Elevated IOP due to impaired aqueous humor drainage through the trabecular pathway is a dominant risk factor for primary open-angle glaucoma (POAG), a leading cause of irreversible blindness.[1] Although IOP is determined by the balance between aqueous humor (AH) secreted by ciliary epithelium and its drainage through the trabecular and uveoscleral pathways, it is the increased resistance to AH drainage through the trabecular meshwork (TM) and Schlemm's canal (SC) that leads to elevated IOP in glaucoma patients.[2,3] Despite continued efforts, our understanding of the molecular and cellular basis of increased resistance to AH outflow in glaucomatous eyes is far from clear.[3] The elevated levels of TGF-β2, endothelin-1 and connective tissue growth factor noted in the AH of glaucoma patients,[3–7] when viewed together with the impairment of AH outflow in experimental studies involving overexpression of or perfusion with some of these factors, argue convincingly for their definitive role in regulation of AH outflow and IOP in normal and glaucomatous eyes.[3,8] Importantly, these observations indicate that alterations in circulating levels and the autocrine and paracrine actions of one or more secreted factors can impact IOP by altering the cellular characteristics of the AH outflow pathway, including the TM, SC, and juxtacanalicular tissue (JCT) with subsequent effects on AH outflow resistance. A mechanistic understanding of the homeostasis of AH outflow resistance in normal eyes and the etiology of elevated IOP in glaucoma patients, therefore, calls for identification and characterization of secretory proteins and extracellular matrix (ECM) protein components of TM cells derived from normal and glaucoma patients, as well as exploration of the role of these proteins in AH outflow. In ongoing proteomics analysis-based studies directed toward this broader goal, we detected the presence of growth differentiation factor-15 (GDF-15) as a common constituent of ECM secreted by human TM cells.[9]

Growth differentiation factor-15 is a divergent member of the TGF-β superfamily involved in a wide range of physiologic and pathologic processes.[10–12] In humans, the *GDF-15* gene maps to chromosome 19p13.1 and the protein is encoded by two exons.[13,14] Growth differentiation factor-15 is synthesized as a 62 kDa pro-precursor, with the mature secreted protein existing as a homodimer of 25 kDa.[11,15] Growth differentiation factor-15 is known to be abundantly produced by the placenta

and expressed at low levels by a variety of tissues and cell types.[12] This pleiotropic cytokine regulates various cellular processes with distinct early and late stage responses during embryogenesis, ageing, and tumorigenesis.[10,12] Growth differentiation factor-15 also is known as a macrophage inhibitory cytokine-1 (MIC-1), prostate-derived factor, placenta TGF-β, and nonsteroidal anti-inflammatory drug activated gene-1.[10,12,15] The physiologic effects of GDF-15 are presumed to be mediated through Type 1 and Type II membrane kinase receptors of the TGF-β family.[12,16] Importantly, serum levels of GDF-15 are increased in a number of different disease states, including cancer, tissue injury, and inflammation.[10,15,17,18] Growth differentiation factor-15 expression is induced by TNF-α, interleukins, P53, Egr-1, and macrophage colony-stimulating factor,[11,15,19–21] with the protein widely being considered a biomarker for various diseases.[11,12,16] Moreover, this cytokine has been shown to interact with connective tissue growth factor and regulate integrin, Rho GTPase, and SMAD signaling activities, and participate in fibrosis and wound healing.[22–28]

Therefore, although GDF-15 has been studied extensively in several other tissues and cell types and is known to be involved in the pathobiology of numerous diseases,[10–12,15,17,29] not much is known regarding the role and regulation of this secreted cytokine in TM cells, AH outflow, and IOP.[30] To explore the role of GDF-15 in TM cell biology, we have, in this initial study, investigated the regulation of GDF-15 expression and effects of this cytokine on human TM cells in the context of AH outflow and IOP.

Methods

Cell Culture

Human TM primary cells were cultured from TM tissue isolated from donor corneal rings used for corneal transplantation at the Duke Ophthalmology Clinical Service, as we described previously.[31] The use of human tissue in this study adhered to the tenets of the declaration of Helsinki. Cells were cultured in plastic petri-plates and six-well dishes maintained at 37°C under 5% CO_2 in Dulbecco's modified Eagle's medium (DMEM) containing 10% fetal bovine serum (FBS), penicillin (100 U/ml)-streptomycin (100 μg/ml) and glutamine (4 mM). All TM cell culture experiments were performed using cells passaged between 3 to 6 times and derived from two human donors (aged 19 and 71 years). All experiments were performed using confluent cell cultures serum starved for 24 hours unless stated otherwise.

RT-PCR and Real-Time Quantitative PCR (RT-qPCR)

Total RNA was extracted from human TM tissue stored in RNAlater (C.No AM7020; Invitrogen, Carlsbad, CA, USA) after dissection from corneal rings obtained from eyes of donors aged 3 and 64 years. Total RNA also was extracted, from cultured human TM cells (control and GDF-15 treated) using the RNeasy Mini Kit (C. No. 74104; Qiagen, Valencia, CA, USA) as we described previously.[31] RNA was quantified using NanoDrop 2000 UV-Vis Spectrophotometer (Thermo Fisher Scientific, Wilmington, DE, USA). Equal amounts of RNA (DNA-free) then were reverse transcribed using the Advantage RT for PCR Kit (C. No. 639506; Clontech Laboratories, Inc., Mountain View, CA, USA) according to the manufacturer's instructions. Polymerase chain reaction amplification was performed on the resultant reverse transcriptase–derived single stranded cDNA using sequence-specific forward and reverse oligonucleotide primers for the indicated genes (Table). For RT-PCR, the amplification was performed using a C1000 Touch Thermocycler (Bio-Rad Laboratories, Hercules, CA, USA) with a standard denaturation, annealing, and extension protocol. The resulting DNA products were separated on 1.5% agarose gels and visualized with GelRed Nucleic Acid Stain (C. No. 41002; Biotium, Hayward, CA, USA) using a Fotodyne Trans-illuminator (Fotodyne, Inc., Hartland, WI, USA).

Real-time qPCR was performed using a CFX 96-RealTime System (Bio-Rad Laboratories), with the aforementioned single stranded cDNA samples. The PCR master mix consisted of 1 μL template cDNA, 10 μL 2 × iQ SYBR Green supermix (C.No. 1708880; Bio-Rad Laboratories), 500 nM each of a gene-specific oligonucleotide pair, and diethylpyrocarbonate-treated water to make up to a total of 20 μL reaction. Briefly, PCR reactions were performed in triplicate using the following protocol: 95°C for 3 minutes followed by 39 cycles of the following sequence: 95°C for 10 seconds (denaturation), 58°C for 30 seconds (annealing), and 72°C for 15 seconds (extension). An extension step was used to measure the increase in fluorescence and melting curves were obtained immediately after amplification. The fold difference in expression of *PRG4*, *SORBS2*, *NCK1*, *ARHGEF2*, *ITGB6*, *VCAN*, *TJAP1*, *FNDC3B*, *DSC2*, *LAYN*, *ATX*, *PARVG*, *SPOCK3*, and *IL1RL1* genes between control and *GDF-15*–treated cells was calculated by the comparative threshold (Ct) method, as described by the manufacturer (CFX Manager; Bio-Rad Laboratories). The cDNA content of control and treated samples for the RT-qPCR reactions was normalized to thelyceraldehyde 3-phosphate dehydrogenase (GAPDH) expression.

Cyclic Mechanical Stretch Studies

Primary cultures of human TM cells were plated on collagen Type 1 BioFlex culture plates with a flexible silicone bottom (C. No. BF-3001C, Flexcell International Corporation, Burlington, NC, USA). As the cells reached confluence, culture medium was switched to serum-free, phenol-free DMEM, and cells were subjected to cyclic mechanical stretch (20% stretching, one cycle per second) for 48 hours, using the computer-controlled, vacuum-operated FX-3000 Flexcell Strain Unit (Flexcell, Hillsborough, NC, USA) as we described previously.[9] Control cells were cultured under similar conditions with no mechanical force applied. Conditioned media were collected from control and stretched cells to analyze GDF-15 protein levels, and RNA was extracted to monitor changes in GDF-15 expression by RT-qPCR analysis.

Immunohistochemistry and Immunofluorescence Analyses

To determine the distribution profile of GDF-15 in the conventional AH outflow pathway, tissue sections from formalin-fixed, paraffin-embedded human eye whole globes (from a 90-year-old donor) were immunostained with GDF-15 antibody as we described previously.[32] Briefly, 5-μm thick tissue sections were deparaffinized and rehydrated using xylene, absolute ethyl alcohol, and water. To unmask antigen epitopes, heat-induced antigen retrieval was performed using 0.1 M citrate buffer pH 6.0 for 20 minutes at 100°C. The slides then were treated with Biocare Medical's Sniper Background Reducer (C. No. BS966; Biocare Medical, Concord, CA, USA) to block nonspecific interactions. Tissue sections then were incubated overnight at 4°C in a humidified chamber with a 1:200 dilution of goat polyclonal primary antibody raised against recombinant (r) human GDF-15 (C.No. AF957, R&D Systems, Inc., Minneapolis, MN, USA). Slides then were washed and incubated with Alexa Fluor-488 donkey anti-goat secondary antibody (Invitrogen/Thermo Fisher Scientific) for 2 hours

Investigative Ophthalmology & Visual Science

Table. Human Oligonucleotide Primers Used in the RT-PCR and RT-PCR Amplifications

Gene Name	Forward Primer	Reverse Primer	Product Size, bps
GDF-15	GGTGAATGGCTCTCAGATG	CACTTCTGGCGTGAGTATC	256
PRG4	GTCCATTCAGTCCACCATCTC	GTCCAGTTAGTCCTCCAAATCC	204
SORBS2	TACCCTGACCCTCCAATAC	CAGCCGTCATCACACTTT	215
NCK1	TGGCTGAGAGAGAGGATGAA	AGATGAGCTGAATGGGTAAAGAG	260
ARHGEF2	CTATACCAATGGGCACCTCTTC	CCCGGATGGTTGTCTTACTTC	248
ITGB6	ACCCTGTCTCCCAAGTAGAA	GATCCGAAGCCCAGTCTAAAG	298
VCAN	CATTCTCCACTGAGCCAACA	CTCCAGAGCCTTCCATCATTAC	252
TJAP1	CTCTTAGCCACAGCTGGATTT	GATCGGCAAACTTGTGGTTTC	219
FNDC3B	CCATCATCTCCCTCCCTATCT	GCTTGCTGTACTGGTCTTCT	209
SPOCK3	CCCACCAGTACAAGCAGAAA	CTGGTCCAATAGCAGGTCATAG	243
DSC2	CCTGAGTGTAACCCTCCAATAC	TGATGGTCTCTGCCTCTCTAT	217
LAYN	GAGCTGACAACACCTGTACTT	CAGATGGTGTGTTGCTTCTTTG	224
ATX	GGGAGACCACGGATTTGATAAC	GGTTGGCCTGAAGGTATTAGTG	214
PARVG	GAGGTGACACAGTCCGAAATAG	CTTCACCACGCTGAGCTTAT	363
IL1RL1	GAAGGCACACCGTAAGACTAAG	GGATTTGTAGTTCCGTGGGTAG	233
ALK1	ATTACCTGGACATCGGCAAC	CACACACACCACCTTCTTCA	254
GAPDH	ACCACAGTCCATGCCATCAC	TCCACCACCCTGTTGCTGTA	452

at room temperature. Immunostained slides then were viewed and imaged using a Nikon Eclipse 90i confocal laser-scanning microscope (Nikon Instruments, Melville, NY, USA) as we described previously.[9] Immunostaining analyses were done in duplicate, and negative controls with no primary antibody were run simultaneously.

Human TM cells grown on gelatin (2%)–coated glass coverslips and treated with rGDF-15 were fixed with 4% paraformaldehyde, permeabilized, blocked, and stained for F-actin with Tetramethylrhodamine (TRITC)-phalloidin (C.No. P1951; Sigma-Aldrich Corp., St. Louis, MO, USA), vinculin with mouse monoclonal anti-vinculin antibody (C.No. V9131; Sigma-Aldrich Corp.), α-smooth muscle actin (αSMA) with mouse monoclonal antibody conjugated with Cy3 (C. No. C6198, Sigma-Aldrich Corp.) and fibronectin with rabbit polyclonal antibody (obtained from Herald Erickson, Duke University), followed by the appropriate secondary antibodies conjugated with Alexa fluorophores, as we described previously.[33] The slides were viewed and imaged using a Nikon Eclipse 90i confocal laser-scanning microscope.

Immunoblotting Analysis

Trabecular meshwork cells subjected to various treatments along with their respective controls were homogenized at 4°C in hypotonic 10 mM Tris buffer, pH 7.4, containing 0.2 mM $MgCl_2$, 5 mM N-ethylmaleimide, 2.0 mM Na_3VO_4, 10 mM NaF, 60 μM phenylmethyl sulfonyl fluoride, 0.4 mM iodoacetamide, and protease and phosphatase inhibitor cocktail (one tablet each/10 ml buffer), using a probe sonicator as we described previously.[31] Protein concentration of cell lysate (800*g* supernatants) and conditioned media (CM) samples was estimated using the Bio-Rad protein assay reagent (C. No. 500-0006, Bio-Rad Laboratories). Samples containing equal amounts of proteins (10 μg for the SDS-urea soluble ECM fraction, cell lysates and CM) were mixed with Laemmli sample buffer and separated using 10% to 12% SDS-PAGE and transferred to nitrocellulose membranes as we described previously.[31] Membranes were blocked for 2 hours at room temperature in Tris buffered saline (TBS) containing 0.1% Tween 20 and 5% (wt/vol) nonfat dry milk and subsequently probed with primary antibodies (at 1:1000 dilution) directed against GDF-15, Hic-5 (mouse monoclonal, C.No. 611164; BD Biosciences, San Jose, CA, USA), phospho-paxillin (polyclonal, C.No. 2541, Cell Signaling Technology, Danvers, MA, USA), phospho-SMAD2/3 (polyclonal, C.No. 8828; Cell Signaling Technology), phospho-SMAD1/5 (polyclonal, C.No. 9516; Cell Signaling Technology), phospho-MLC (polyclonal, C.No. 3674; Cell Signaling Technology); MLC (polyclonal, C.No. 3672; Cell Signaling Technology), phospho-MYPT1 (polyclonal, C.No. ABS45; Millipore, Billerica, MA, USA), αSMA (monoclonal, A2547, Sigma-Aldrich Corp.), fibronectin (1:15000 dilution; polyclonal C.No. ab23750; Abcam, Cambridge, MA, USA), and GAPDH (mouse monoclonal antibody at 1:10000 dilution; C. No. 60004-1-g, Proteintech Group, Inc. Rosemont, IL, USA), in conjunction with horseradish peroxidase-conjugated secondary antibodies. Detection of immunoreactivity was based on enhanced chemiluminescence. Densitometric analysis of the immunoblots was performed using ImageJ software (available in the public domain at http://imagej.nih.gov/ij/; provided in the public domain by the National Institutes of Health (NIH), Bethesda, MD, USA). Data were normalized to the specified loading controls. Urea-glycerol gels were used for phospho-MLC immunoblots, as we described previously.[33]

cDNA Microarray Analysis

Human TM cells from 19-year-old donor eyes (passage 4) were cultured to confluence, serum-starved for 24 hours, and treated with 20 ng/ml GDF-15 (prepared in sterile 4 mM HCl) for 24 hours, along with control cells treated with an equal volume of 4 mM HCl. Briefly, cells were shredded using the QiaShredder (C. No. 79654; Qiagen) column and treated with DNAse I to eliminate genomic DNA contamination. Total RNA then was extracted using the RNeasy Mini kit (Qiagen) according to the manufacturer's instructions. Purified RNA was quantitated using a Nanodrop 2000 Spectrophotometer and subjected to cDNA microarray analysis at the Duke Microarray Core facility (Duke National Cancer Institute and Duke Genomic and Computational Biology shared resource facility, Durham, NC, USA). Briefly, RNA quality was assessed using an Agilent 2100 Bioanalyzer G2939A (Agilent Technologies, Santa Clara, CA, USA) and Nanodrop 8000 Spectrophotometer. Hybridization targets were prepared from total RNA using a MessageAmp Premier RNA Amplification Kit (Applied Biosystems/Ambion, Austin, TX, USA), hybridized to GeneChip Human Genome U133 Plus 2 (Affymetrix, Santa Clara, CA, USA) arrays in an Affymetrix GeneChip hybridization Oven

Investigative Ophthalmology & Visual Science

645, washed in Affymetrix GeneChip Fluidics Station 450, and scanned with Affymetrix GeneChip Scanner 7G according to standard Affymetrix GeneChip hybridization, wash, and stain protocols. Raw data were normalized and analyzed using GeneSpring 10 (Silicon Genetics, Wilmington, DE, USA). The genes were filtered by intensity compared to the control channel, and a P value of ≤ 0.05 by the paired Student's t-test was considered significant. A list of selected genes (Table) that were upregulated by GDF-15 (minimum of 2-fold) based on cDNA microarray was independently confirmed by RT-qPCR.

Extraction of ECM-Enriched Fraction

Human TM cells were plated on 100 × 20 mm Eppendorf plastic cell culture dishes (C. No. 0030702115) in DMEM with 10% FBS. After cells reached confluence, the growth medium was changed to serum-free medium, and cells were serum starved for 24 hours. These cultures were treated with GDF-15 (20 ng/ml) on a daily basis for 48 hours. The ECM was extracted as we described previously using Triton X-100, ammonium hydroxide, and DNase-I.[9] The ECM was solubilized as described previously,[34] with 200 µl of SDS buffer containing 5% SDS, 10% glycerol, 60 mM Tris-HCL, pH 6.8. The SDS-lysate was collected into 1.7-ml microcentrifuge tubes (Axygen, Union City, CA, USA), incubated at 95°C for 5 minutes, with gentle mixing and spun down at 16,000g for 10 minutes. The supernatant containing SDS-soluble ECM proteins were transferred to a clear tube and placed on ice. The protein pellets (termed SDS-insoluble fraction) were processed further by adding urea buffer containing 8 M urea, 4% SDS, 60 mM Tris-HCl, and 12.5 mM EDTA. The pellet was pipetted repeatedly to facilitate resuspension and allowed to sit for 30 minutes at room temperature to enhance complete solubilization in urea buffer and spun down at 16,000g for 5 minutes at room temperature. The supernatant from this step was combined with the SDS-soluble fraction to generate a SDS/urea-soluble fraction, which was stored at −80°C until further analysis. The protein concentration of the SDS-urea soluble ECM fraction was measured using the Micro BCA Protein Assay Kit (C. No. 23235; Pierce Biotechnology, Rockford, IL) according to manufacturer's protocol.

In-Gel Protein Digestion

After protein estimation, each ECM-enriched sample described above was loaded into a 1.5 mm 4% to 20% gradient Tris-Glycine gel (Bio-Rad Laboratories) along with a prestained protein molecular weight ladder (Thermo Fisher Scientific). Samples were electrophoresed at 200 V for 30 to 45 minutes using 2-(N-morpholino) ethanesulfonic acid (MES)-SDS running buffer (Novex Invitrogen). The gel was stained overnight with gel code blue stain reagent (C. No. 24590; Pierce Biotechnology) and destained using deionized water at 4°C. After destaining with deionized water, protein bands were excised from the gel and subjected to in-gel tryptic digestion using Trypsin/Lys-C mix 1 µg (C. No. V5072; Promega, Madison, WI, USA) and the In-Gel Tryptic digestion kit (Pierce Biotechnology), as per manufacturer's instructions. This digestion process included reduction and alkylation of protein samples.

Mass Spectrometry

Briefly, trypsin digested ECM peptides were extracted from gel slices using 250 µl of 50% acetonitrile/1% formic acid at 38°C for 40 minutes. These peptide samples were transferred into a new, 0.5-ml centrifuge tube, dried by SpeedVac (Thermo Fisher Scientific) and resuspended in 10 µl of 0.1% formic acid. Three µL aliquots of tryptic digests were analyzed by liquid chromatography–tandem mass spectrometry (LC-MS/MS) using a nanoAcquity UPLC system coupled to a Synapt G2 HDMS mass spectrometer (Waters Corp., Milford, MA, USA). Peptides were initially trapped on a 180 µm × 20 mm Symmetry C18 column (at the 5 µL/min flow rate for 3 minutes in 99.9% water, 0.1% formic acid). Peptide separation then was performed on a 75 µm × 150 mm column filled with the 1.7 µm C18 BEH resin (Waters Corp.) using the 6% to 30% acetonitrile gradient with 0.1% formic acid for 1 hour at the flow rate of 0.3 µL/minute at 35°C. Eluted peptides were sprayed into the ion source of Synapt G2 using the 10 µm PicoTip emitter (Waters Corp) at the voltage of 2.5 kV.

For each sample we conducted a data-dependent analysis (DDA) using a 0.8-second MS scan followed by MS/MS acquisition on the top four ions with charge greater than one. Tandem mass spectrometry scans for each ion used an isolation window of approximately 3 Da, a maximum of 2 seconds per precursor, and dynamic exclusion for 90 seconds within 1.2 Da. Data-dependent analysis data were converted to searchable files using ProteinLynx Global Server 2.5.1 (Waters Corp.) and searched against the human UniProt database (September 2015 release), using Mascot server 2.2 with the following parameters: maximum one missed cleavage site, carbamidomethylation at Cys residues as fixed modification, and Met oxidation, Asn, Gln deamidation as variable modifications. Precursor ion mass tolerance was set to 20 ppm, while fragment mass tolerance to 0.2 Da. Mascot data were imported into Scaffold 4.4 (Proteome Software, Inc., Portland, OR, USA) to arrange all the data sets, identify a false discovery rate for protein identification, group proteins, and perform spectral counting–based protein quantification. Acceptance criteria for protein identification required identification at least two peptides for each protein with a confidence interval percentage (CI%) over 99.0%, corresponding to a false discovery rate of 1%. Complete mass spectrometry analysis was performed with two independently obtained SDS-Urea soluble ECM preparations.

Statistical Analysis

Statistical analysis was performed using GraphPad Prism version 7 for Windows (GraphPad Software, La Jolla, CA, USA). All data represent the average results of at least four independent experiments unless otherwise mentioned. One-way ANOVA with Bonferroni's multiple comparisons test was done for comparing within groups and Student's t-test was used for all other statistical comparison between two groups. A P value of ≤ 0.05 was considered statistically significant.

Results

Expression and Distribution of GDF-15 in TM Cells and Tissue

To determine the expression of GDF-15 in TM cells and tissue, we initially performed RT-PCR analysis using total RNA extracted from human TM primary cell cultures and tissue and gene-specific oligonucleotide PCR primers. Figure 1A shows amplification of a GDF-15–specific DNA product of the expected size from primary TM cell cultures derived from multiple human donor specimens and two independent human TM tissue samples. The identity of the PCR product as a GDF-15–specific DNA fragment was confirmed by sequence analysis. Having confirmed *GDF-15* gene expression in TM cells and tissue, we then evaluated presence of GDF-15 protein product in the human TM cell ECM fraction, lysates, and CM using a polyclonal goat antibody raised against a full

Investigative Ophthalmology & Visual Science

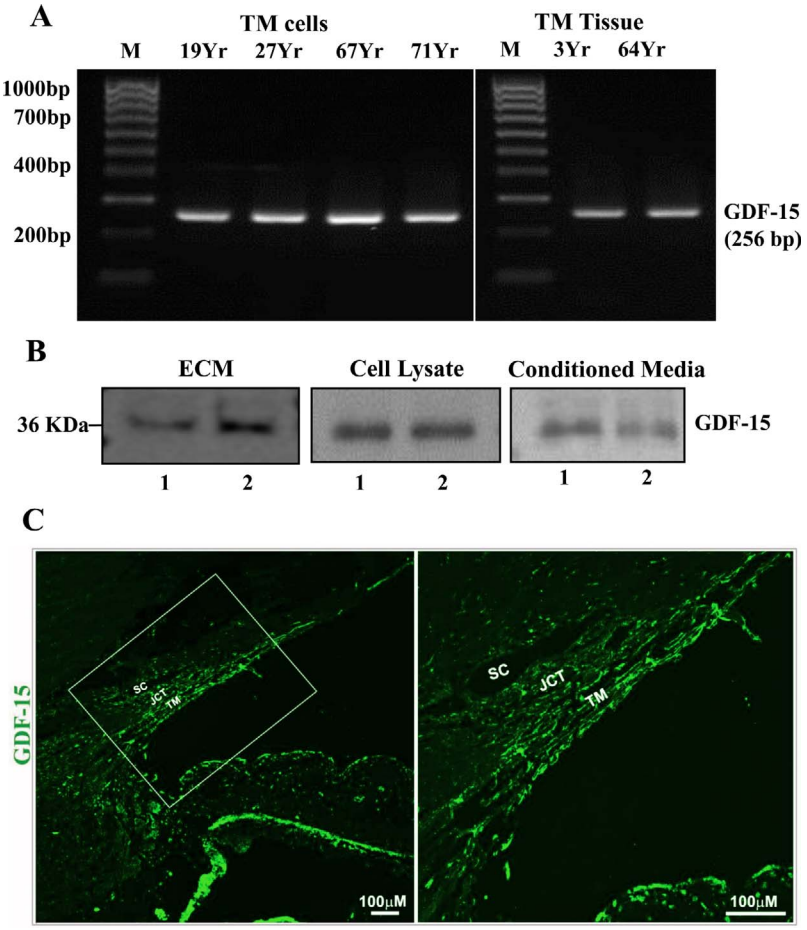

Figure 1. Expression and distribution of GDF-15 in human TM cells, tissue, and the AH outflow pathway. (**A**) Reverse transcription-PCR based detection of GDF-15 expression in TM cells derived from several individual human donor eyes and TM tissue. (**B**) Immunoblotting-based detection of GDF-15 protein in the SDS-urea soluble ECM fraction, cell lysates, and conditioned media from two independent primary cultures of human TM cells (lanes *1*, *2*). (**C**) Immunofluorescence (*green*)–based analysis of GDF-15 distribution in the human AH outflow pathway. The panel on the *right* shows a magnified image of the boxed portion in the *left* panel. *Scale bars*: Indicate image magnification.

length recombinant human GDF-15. As shown in Figure 1B, the SDS-urea soluble TM cell ECM fraction (10 μg protein),[9] TM cell lysates, and CM (10 μg protein per sample) derived from two independent samples (Fig. 1B, lanes 1 and 2) exhibited a single immunopositive band of expected size (~36 kDa, based on the antibody provider's data sheet; R&D Systems, Inc.). Following these observations, we also assessed the distribution profile of GDF-15 protein in the human AH outflow pathway by immunohistochemical analysis of paraffin-embedded human donor eye tissue sections (from a 90-year-old donor). Figure 1C shows the distribution of GDF-15 throughout the conventional AH outflow pathway with high immunofluorescence staining intensity noted in the TM relative to SC and JCT (Fig. 1C, green). Tissue specimens stained simultaneously with Alexa Fluor 488 conjugated secondary antibody alone did not exhibit detectable fluorescence (data not shown).

Regulation of GDF-15 Expression in Human TM Cells

To identify regulatory inputs controlling GDF-15 expression in TM cells, we evaluated the effects of physiologic agents, including TGF-β2, dexamethasone, lysophosphatidic acid (LPA), endothelin-1, TNF-α, and IL-1β, all of which have been demonstrated to influence IOP and AH outflow in experimental studies.[3,7,35,36] All treatments were performed using confluent cultures of primary human TM cells derived from two different donors (19 and 71 years old), and maintained under serum-free conditions for 24 hours before treatment with the appropriate recombinant protein or high grade reagent obtained from commercial sources. Human TM cells treated with TGF-β2 (10 ng/ml, 24 hours; C.No. T2815, Sigma-Aldrich Corp.), dexamethasone (0.5 μM, daily for 4 days; C.No. D4902; Sigma-Aldrich Corp.), endothelin-1 (2 μM/24 hours; C.No. E7764; Sigma-Aldrich Corp.), LPA (5 μM/6 hours; C.No. SC-201053; Santa Cruz Biotechnology, Santa Cruz, CA, USA), IL-1β (10 ng/ml, 24 hours; C.No. 554602 ; BD Biosciences), or TNF-α (10 ng/ml, 24 hours; C.No. 210-TA; R&D Systems, Inc.) exhibited a significant increase in GDF-15 protein levels in cell lysates as determined by immunoblot analyses with subsequent densitometric quantification (Figs. 2A, 2C, 2E, 2F). All immunoblots presented in Figure 2 show data from two independent representative samples per treatment, with the densitometric data being derived from four independent samples. Values are shown as mean ± SEM. Glyceraldehyde-3-phosphate dehydrogenase was immunoblotted to normalize protein loading for the cell lysate samples. In addition to the results obtained with cell lysates, CM from TGF-β2 and dexamethasone-treated TM cells also revealed a significant increase in GDF-15 levels compared to control cells (Figs. 2B, 2D). To control for protein loading of CM samples,

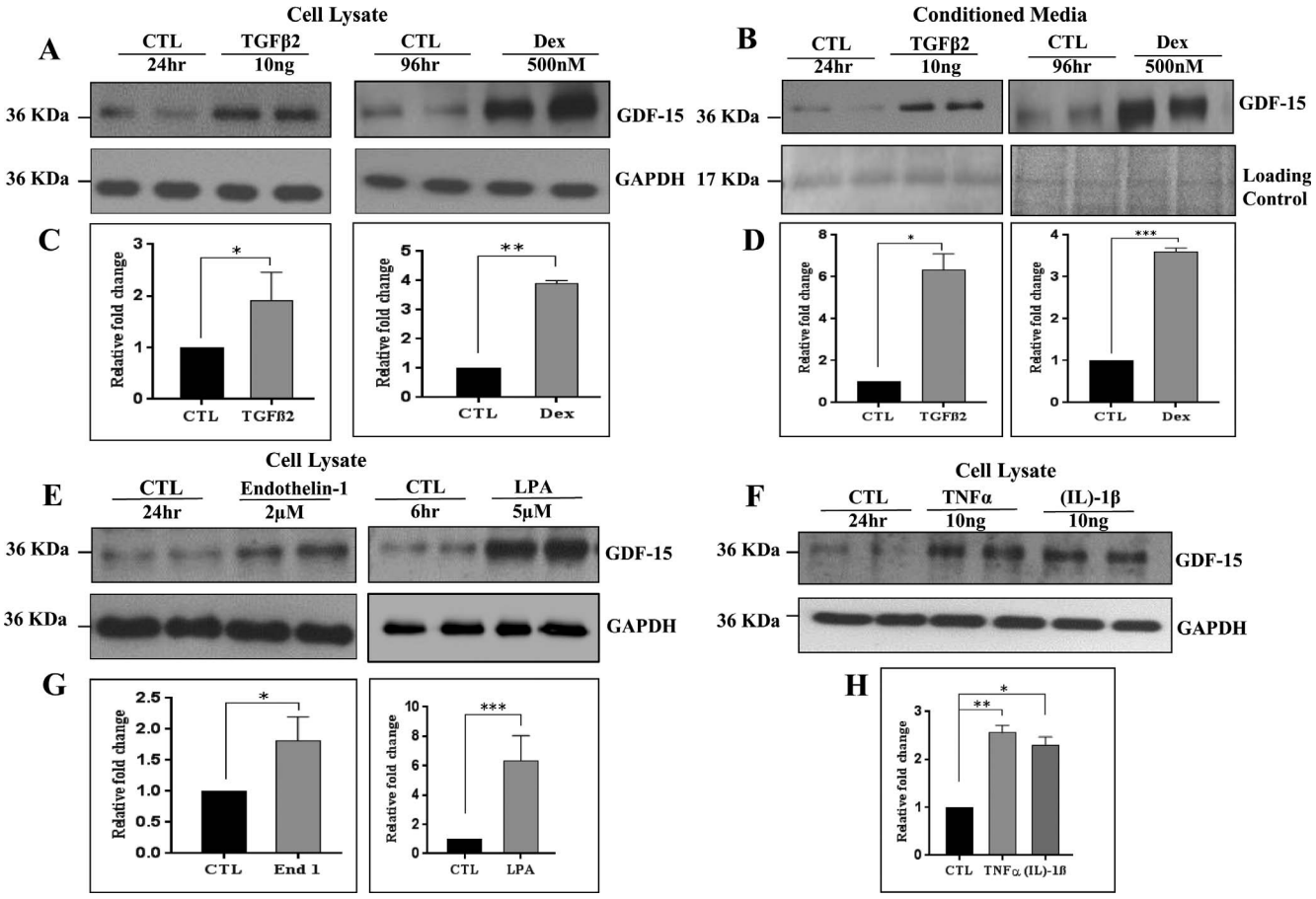

Figure 2. Regulation of GDF-15 protein levels in human TM cells. (**A**, **C**, **E**–**H**). Confluent serum-starved TM cells treated with TGFβ2 (10 ng/ml, 24 hours), dexamethasone (500 nM/4 days), endothelin-1 (2 μM/24 hours), LPA (5 μM/6 hours), TNFα (10 ng/ml, 24 hours), and IL-1β (10 ng/ml, 24 hours) showed a significant increase in GDF-15 protein levels in cell lysates compared to control cells (CTL) based on immunoblot analysis. (**B**, **D**) Similarly, conditioned media derived from the TGF-β2 and dexamethasone treated TM cells showed a significant increase in GDF-15 protein levels compared to control cells. Histograms depict the fold change in GDF-15 protein levels in the above described samples compared to controls based on densitometric analysis. Glyceraldehyde-3-phosphate dehydrogenase was immunoblotted as a loading control for the cell lysates. Protein loading was normalized for conditioned media samples by subjecting the equal amounts of protein to SDS-PAGE analysis and staining with gel code blue. Staining intensity of the indicated protein band (17 kDa) was used for normalization. Values represent the mean ± SEM of 4 independent determinations. $^{*}P \leq 0.05$; $^{**}P \leq 0.01$; $^{***}P \leq 0.001$.

equal amounts of CM protein (10 μg) were separated by SDS-PAGE and stained with gel code blue and as shown in Figure 2B, the intensity of one of the protein bands (17 kDa) was used to normalize protein loading between the treated and control samples.

We then assessed the effects of mechanical stretch on GDF-15 protein levels since TM is a well characterized mechano-sensing tissue.[37,38] To this end, confluent human TM cells cultured on collagen Type I BioFlex culture plates with a flexible silicone bottom were maintained under serum-free conditions for 24 hours and then subjected to 20% cyclic mechanical stretch for 48 hours. The CM derived from these samples was analyzed by immunoblotting to determine changes in the level of GDF-15 protein, while RNA was extracted to monitor for changes in *GDF-15* gene expression by RT-qPCR analysis. As shown in Figure 3, *GDF-15* expression in TM cells underwent a robust and significant increase at the translational (Figs. 3A, 3B) and transcriptional levels (Fig. 3C), in response to cyclic mechanical stretch. In Figure 3A, data from three independent representative samples were shown along with a loading control. The quantitative data shown in Figures 3B and 3C is based on six and three independent analyses, respectively.

GDF-15–Induced Changes in TM Cell Gene Expression

To seek broader insight into the role of GDF-15 in TM cells, we evaluated initially the effects of human rGDF-15 (C.No. 957-GD-025/CF; R&D Systems, Inc.) on gene expression by cDNA microarray analysis. The Affymetrix GeneChip Human Genome U133 Plus 2 array, which represents 38,500 well-induced changes, characterized human genes, and is comprised of more than 54,000 probe sets, was used for this purpose. Trabecular meshwork cells (passage 4) derived from a 19-year-old human donor eye were grown to confluence in Eppendorf plastic petri-plates, serum starved for 24 hours, and treated with rGDF-15 (20 ng) for 24 hours. Total RNA extracted from the control and rGDF-15 treated samples was subjected to cDNA microarray analysis as described in the Methods section. In this pilot experiment, based on a single sample of cDNA microarray analysis, we detected a minimum of a 2-fold increase in the expression level of a total of 475 individual genes in GDF-15–treated cells relative to control cells (Supplementary Table S1). In contrast to the large number of genes which exhibited upregulated expression, a smaller number (<70 genes) revealed a decrease in expression level (maximum of a 2-fold decrease) in GDF-15–stimulated cells relative to corresponding

Investigative Ophthalmology & Visual Science

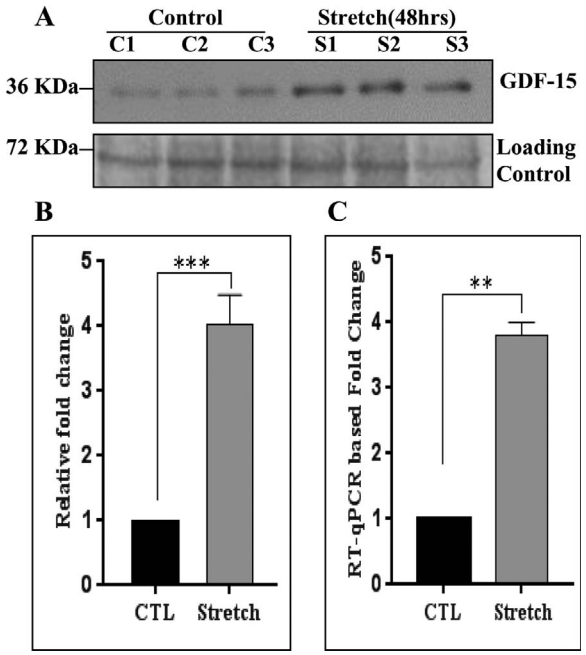

Figure 3. Effect of cyclic mechanical stretch on regulation of GDF-15 expression in human TM cells. (**A**) Conditioned media derived from human TM cells subjected to cyclic mechanical stretch (20% stretch, 1 cycle/sec for 48 hours) under serum-free conditions exhibited a significant increase in the GDF-15 protein levels compared to controls based on immunoblot analysis. (**B**) Histograms depict the fold change in GDF-15 protein levels in stretched TM cells relative to controls based on densitometric analysis. For loading control, conditioned media samples were subjected to SDS-PAGE and gel code *blue* staining, followed by the use of staining intensity of indicated protein bands for normalization. Values are mean ± SEM of six independent analyses. (**C**) RNA derived from TM cells subjected to cyclic mechanical stretch along with their respective controls as described above was analyzed for changes in GDF-15 expression by RT-qPCR. The stretched cells revealed a significant increase in GDF-15 expression compared to control cells. Values (mean ± SEM) are based on three independent analyses. $^{**}P \leq 0.01$, $^{***}P \leq 0.001$.

controls (Supplementary Table S2). Ingenuity Platform Pathway analysis (IPA; Qiagen) indicates that of the genes exhibiting GDF-15–dependent upregulation in expression, several encode ECM, chaperones, intracellular signaling proteins, and those involved in cell survival, death, connective tissue development and function, morphology, adhesion, cell junctions, Rho GTPase signaling, and cytoskeletal organization (Supplementary Table S1).

To confirm the results of cDNA microarray analysis by an independent approach, we used RT-qPCR to evaluate expression of selected representative genes whose levels were upregulated between 2- and 20-fold relative to controls. Trabecular meshwork cells derived from 19- and 71-year-old human donors were used for this experiment, and treated with rGDF-15 (20 ng/ml) for 24 hours as described above, before RNA extraction (triplicate samples from two independent TM cell strains) and RT-qPCR analysis. Figure 4 shows the significant increase in expression levels for most genes evaluated (see Figs. 4A–C), in GDF-15–treated cells. This subset of genes included sorbin and SH3 domain containing 2 (SORBS2), proteoglycan 4 (PRG4), NCK-associated protein 1 (NCK1), versican (VCAN), tight junction–associated protein 1 (TJAP1), fibronectin type III domain containing 3B (FNDC3B), desmocollin 2 (DSC2), Sparc/osteonectin, cwcv and kazal-like domains proteoglycan 3 (SPOCK3), layilin (LAYN), autotaxin

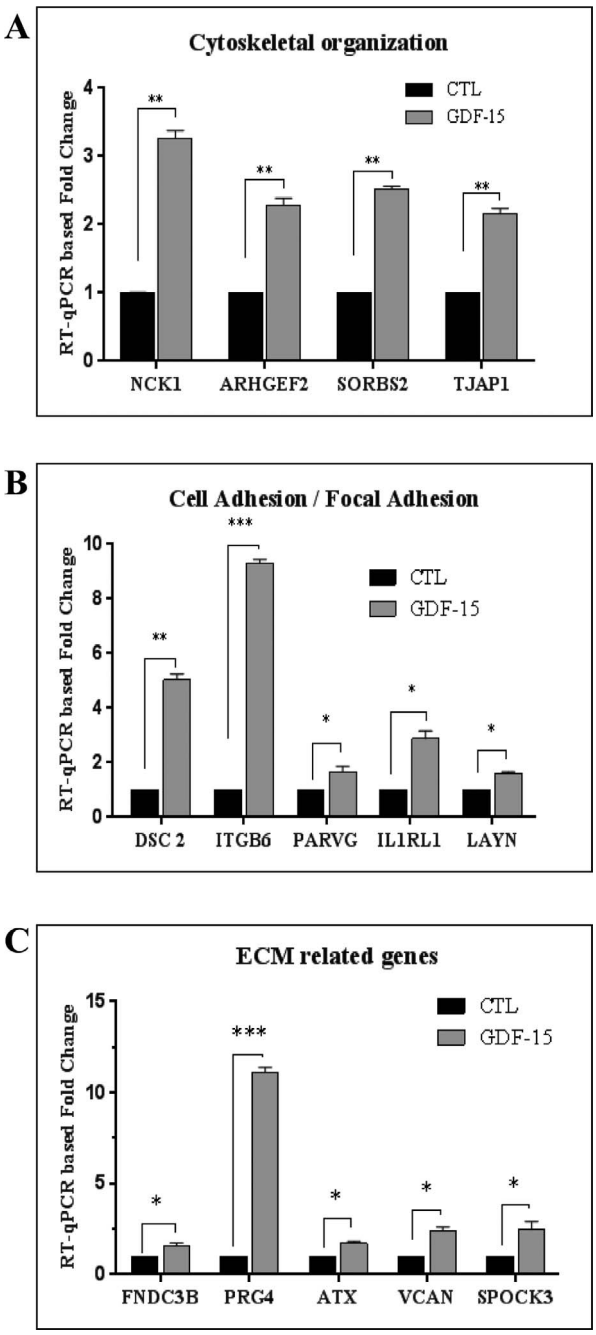

Figure 4. Real-time qPCR–based confirmation of GDF-15–induced gene expression in human TM cells. An RT-qPCR–based approach was undertaken to independently validate the data obtained from cDNA microarray analyses of the effects of GDF-15 on gene expression in TM cells. A portion of the RNA submitted for cDNA microarray analysis was reverse transcribed and used for the RT-qPCR experiment along with another biologic replicate of TM cells derived from a 71-year-old donor. The selected genes were categorized based on their Gene Ontology terms and clustered into three different groups namely; (**A**) Cytoskeletal organization (*NCK1*, *ARHGEF2*, *SORBS2*, and *TJAP1*), (**B**) Cell adhesion (*DSC2*, *ITGB6*, *PARVG*, *IL1RL1*, and *LAYN*), and (**C**) ECM-related genes (*FNDC3B*, *PRG4*, *ATX*, *SPOCK3*, and *VCAN*). Real-time quantification of the expression of selected genes was normalized to the cycle values of *GAPDH*. Fold changes were calculated based on the values from triplicate analyses of two individual samples ($n = 6$, mean ± SEM). The selected genes showed a significant increase (in fold change) in expression upon GDF-15 treatment as compared to corresponding controls. $^{*}P \leq 0.05$; $^{**}P \leq 0.01$; $^{***}P \leq 0.001$.

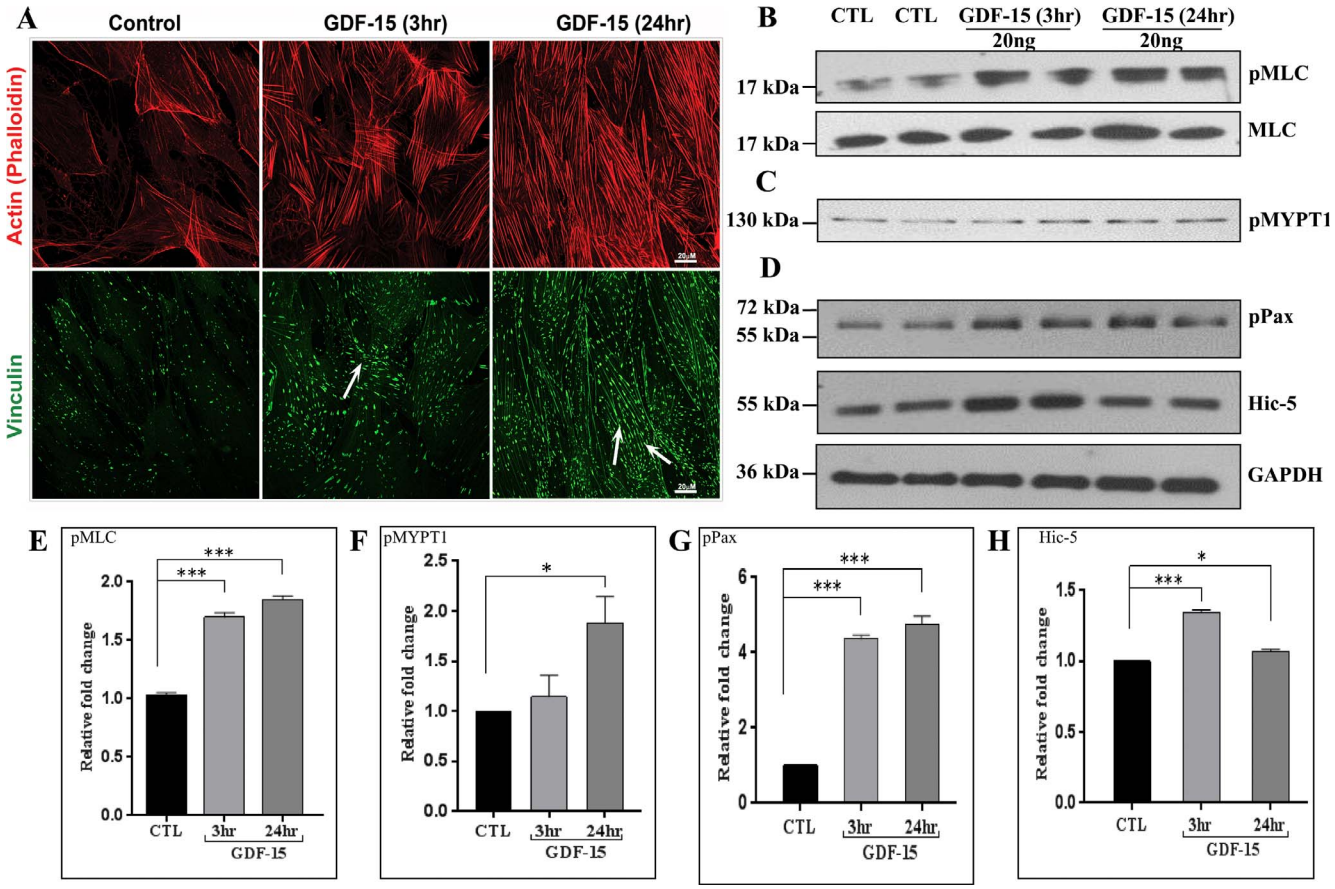

Figure 5. Growth differentiation factor-15 induces actin stress fibers and focal adhesion and alters contractile properties of human TM cells. (**A**) Human TM cells cultured on 2% gelatin-coated glass cover slips and serum-starved for 24 hours were treated with GDF-15 (20 ng/ml for 3 and 24 hours) before staining for F-actin and focal adhesion protein- vinculin with TRITC-phalloidin and vinculin antibody in conjunction with Alexa fluor-488 conjugated secondary antibody, respectively. Representative confocal images of stained cells revealed a time dependent increase in actin stress fibers (*red*) and focal adhesions (*green*, *arrows*) with GDF-15 treatment. Trabecular meshwork cells treated with GDF-15 exhibited a significant increase in the levels of phosphorylated-MLC (**B**), MYPT1 (**C**), and paxillin, and Hic-5 (**D**) relative to CTL based on immunoblot analysis. The immunoblot data were normalized to total MLC (for pMLC) and GAPDH (for p-paxillin, Hic-5, and pMYPT1). Histograms (**E**–**H**) depict the fold change in the levels of indicated proteins based on densitometric analysis. Values represent mean ± SEM. $n = 4$, $^{*}P \leq 0.05$; $^{***}P \leq 0.001$.

(ATX), IL-1 receptor-like 1 (IL1RL1), integrin β6 (ITGB6), Rho guanine exchange factor (ARHGEF2), and gamma parvin (PARVG). Thus, the RT-qPCR–based results were consistent with data from cDNA microarray analysis, as described above.

Regulation of TM Cell Contractile and Adhesive Characteristics by GDF-15

The ability of GDF-15 to increase expression of genes encoding proteins involved in cytoskeletal and cell adhesion changes, together with the known effects of contractile and cell adhesive properties of TM cells on AH outflow and IOP,[7,39] led us to test a possible role for GDF-15 in TM cell actin cytoskeletal organization and focal adhesion formation. Serum-starved quiescent TM cells treated with rGDF-15 (20 ng/ml) exhibited a progressive and time-dependent increase in formation of actin stress fibers and focal adhesions, relative to control cells (Fig. 5A). We then examined the effects of rGDF-15 on phosphorylation of MLC and myosin phosphatase target subunit 1 (MYPT1) in TM cells, given that these proteins are key regulators of actomyosin interactions and contractile properties of cells.[40] Immunoblotting followed by quantitative densitometric analyses of serum-starved confluent human TM cells treated with rGDF-15 (20 ng/ml) revealed significant increases in levels of pMLC by 3 hours post addition with no changes in total MLC. This increase was sustained even at 24 hours relative to untreated control TM cells (Figs. 5B, 5E). A significant increase also was noted in the levels of pMYPT1, but only after 24 hours of stimulation of TM cells with rGDF-15 (Figs. 5C, 5F). Under these conditions, the levels of phosphorylated paxillin, a key regulator of cell adhesion and Hic-5, another well characterized paxillin-related cell adhesion protein[41] also were significantly increased by 3 hours of rGDF-15 treatment (Fig. 5D). However, while the levels of phosphorylated paxillin remained elevated at 24 hours, no changes were noted in Hic-5 levels between rGDF-15–treated cells and control cells (Figs. 5G, 5H). These observations taken together revealed that GDF-15 regulates TM cell contractile and cell adhesive properties.

Cell contractile and adhesive properties are known to influence expression of αSMA and ECM encoding genes especially in the endothelial and mesenchymal cells.[31,42] In light of the knowledge that GDF-15 has been shown to induce fibrotic activity,[27,28,43] we then examined the effects of rGDF-15 on protein levels of αSMA and fibronectin in human TM cells, using immunofluorescence and immunoblot analyses. Serum-starved TM cells treated with rGDF-15 (20 ng/ml) for 3 and 24 hours showed a robust and progressive increase in immunostaining for αSMA and fibronectin compared to

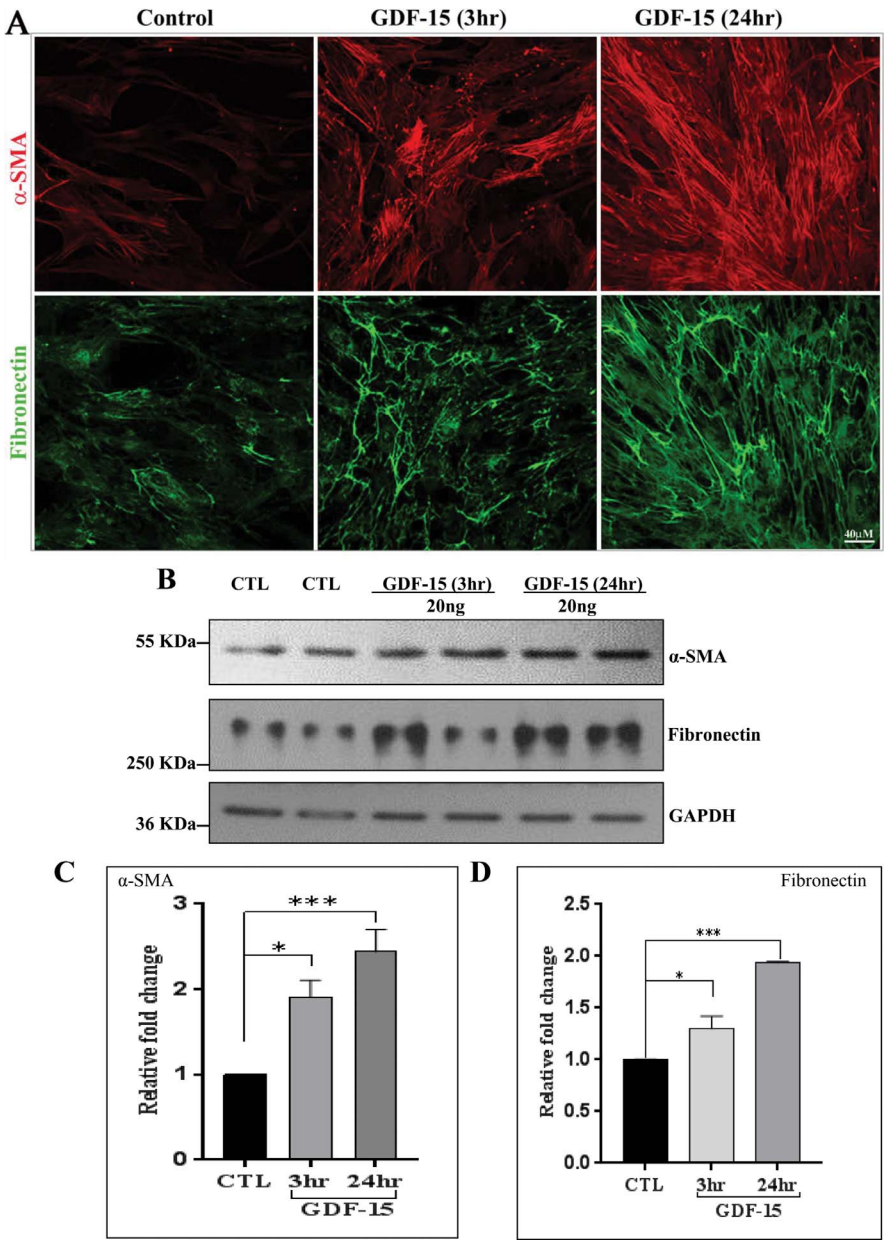

Figure 6. Growth differentiation factor-15 increases the levels of αSMA and fibronectin in human TM cells. (**A**) Human TM cells were grown on 2% gelatin-coated glass cover slips, serum-starved for 24 hours and treated with GDF-15 (20 ng/ml for 3 and 24 hours). Following fixation, cells were immunostained for α-SMA (*red*) and fibronectin (*green*). Representative confocal images of stained cells show a progressive increase in α-SMA and fibronectin specific immunofluorescence upon GDF-15 treatment compared to control cells. (**B**). Immunoblot analysis confirmed that GDF-15–treated human TM cells exhibit increased levels of α-SMA and fibronectin compared to CTL. The immunoblot data were normalized to GAPDH. (**C**, **D**). Histograms depict the fold change in the levels of αSMA and fibronectin in TM cells treated with GDF-15 treatment, based on densitometric analysis. Values are mean ± SEM. $n = 4$, $^{*}P \leq 0.05$; $^{***}P \leq 0.001$.

control cells (Fig. 6A). Consistent with these observations, immunoblotting analysis for αSMA and fibronectin confirmed a significant and time-dependent increase in protein levels at 3 and 24 hours of treatment with rGDF-15 treatment (Figs. 6B–D).

Role for SMAD and Rho Kinase in GDF-15–Induced Myosin Light Chain Phosphorylation in TM Cells

To identify the intracellular signaling pathways mediating the effects of GDF-15 on MLC phosphorylation in TM cells (Fig. 5), we used inhibitors of Rho kinase and SMAD3. Since GDF-15 is a TGF-β–related cytokine, and the fibrogenic activity of TGF-β is linked to its known effects on cell contractile activity and MLC phosphorylatyion,[31] we compared the relative effects of GDF-15 and TGF-β2 on MLC phosphorylation in TM cells. Treatment of serum-starved TM cells treated with 10 ng/ml of GDF-15 or TGF-β2 for 24 hours significantly increased MLC phosphorylation, with TGF-β2 stimulating a significantly stronger response than GDF-15, as shown in Figures 7A and 7C. Total MLC was probed as a loading control, the levels of which were not affected either by GDF-15 or TGF-β2 treatment. Although GDF-15– and TGF-β2–treated samples were analyzed on the same gel (Fig. 7A) for purposes of evaluating changes in pMLC, other samples treated with different concentrations of GDF-15

Investigative Ophthalmology & Visual Science

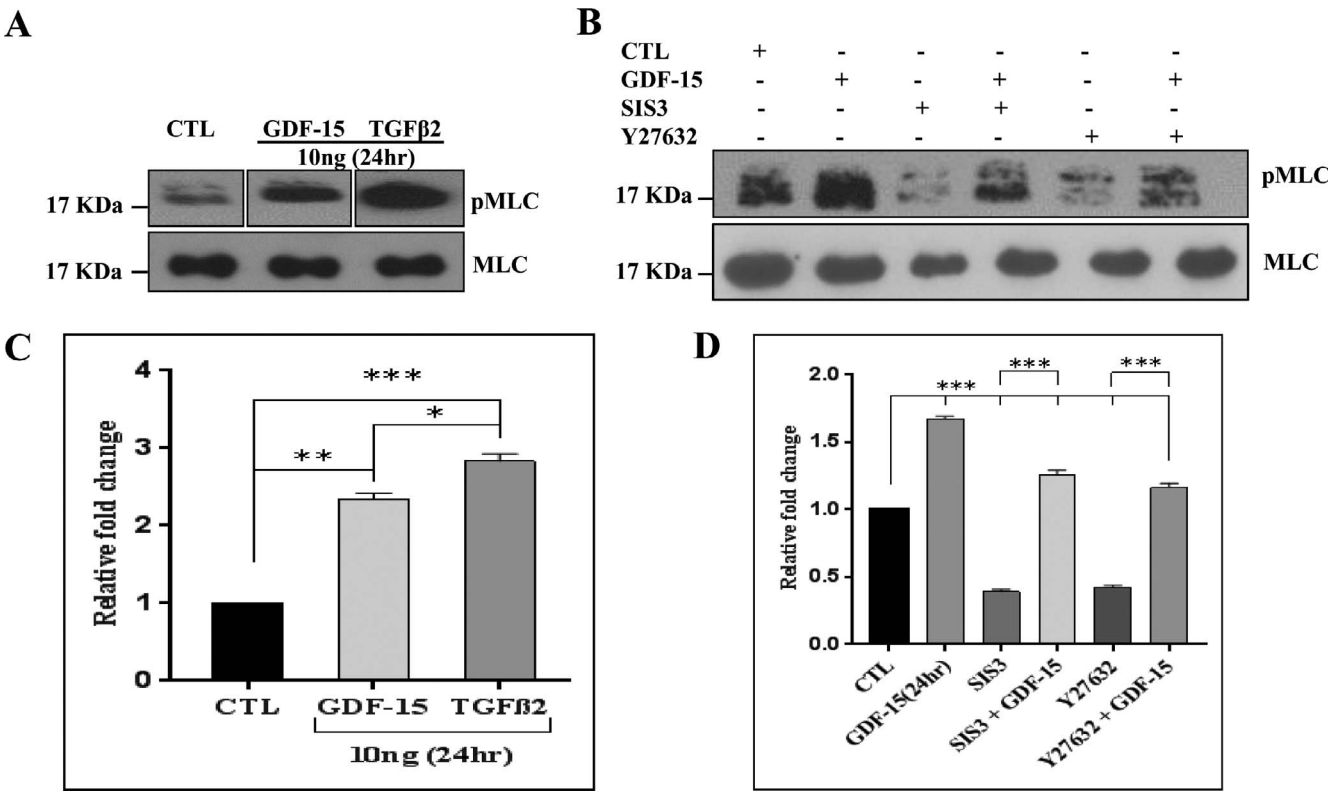

Figure 7. Comparison of the effects of GDF-15 and TGF-β2 and inhibitors of SMAD3 and Rho kinase on MLC phosphorylation in TM cells. (**A**) Serum starved human TM cells were treated either with GDF-15 or with TGF-β2 (10 ng/ml for 24 hours) and analyzed for changes in the level of MLC phosphorylation in a comparative manner along with their respective controls. The quantitative immunoblot data revealed that while GDF-15 and TGF-β2 significantly increased MLC phosphorylation, the magnitude of response with TGF-β2 was relatively much stronger than that triggered by GDF-15 (**C**). (**B**, **D**) Serum-starved TM cells treated with GDF-15 (20 ng/ml for 24 hours) alone or in the presence of SMAD3 inhibitor-SIS3 or Rho kinase inhibitor- Y27632 (10 μM for 6-hour pretreatment) or with inhibitors alone showed a dramatic and significant decrease in MLC phosphorylation in samples treated with inhibitors (SIS3 or Y-27632) alone and this response was partially rescued by GDF-15 but significantly less than GDF-15 alone based on immunoblot with subsequent densitometry based quantification. Total MLC was immunoblotted as a loading control. Values are shown as mean ± SEM. $n = 4$. $^{*}P \leq 0.05$; $^{**}P \leq 0.01$; $^{***}P \leq 0.001$.

were run between sample sets treated with 10 ng of either the GDF-15 or TGF-β2. This necessitated cropping of blots to support a side-by-side analysis of pMLC levels in cells treated with 10 ng of GDF-15 or TGF-β2.

In a separate experiment we tested the effects of SMAD 3 inhibitor SIS3 and Rho kinase inhibitor Y-27632 in the presence and absence of GDF-15 on MLC phosphorylation in TM cells, to determine whether SMAD3 or Rho kinase or both involved in GDF-15–induced contractile activity. As shown in Figures 7B and 7D, serum-starved TM cells treated with 10 μM SIS3 or Y27632 for 6 hours significantly decreased the levels of pMLC compared to the controls. On the other hand, addition of GDF-15 (20 ng/ml for 24 hours) following pretreatment with either SIS3 or Y-27632 for 6 hours (10 μM), rescued partially the inhibition of MLC phosphorylation induced by SIS3 and Y-27632 but not completely (Fig. 7B). The levels of pMLC in the TM cells treated either with SMAD3 inhibitor or Rho kinase inhibitor in the presence of GDF-15 were significantly lower than the levels observed with GDF-15 alone, indicating a putative role of SMAD3 and Rho kinase in GDF-15–induced TM cell contractile activity (Figs. 7B, 7D).

Activation of SMAD Signaling by GDF-15 in TM Cells

Since the GDF-15–induced MLC phosphorylation in TM cells was dependent on SMAD signaling (Fig. 7B), we asked whether GDF-15 activated SMAD signaling in TM cells. For this, serum-starved TM cells were challenged with rGDF-15 (20 ng/ml) for 3 and 24 hours before analysis of changes in the levels of phosphorylated SMAD 2/3 and SMAD 1/5 by immunoblot analysis, using the appropriate phospho-specific antibodies. Phosphorylation of SMAD2 was significantly induced by 3 hours of stimulation and this increase was sustained up to 24 hours following rGDF-15 addition to TM cells. While SMAD3 phosphorylation also was significantly increased in response to GDF-15, the magnitude of increase was at a much lower level relative to activation of SMAD2 (Fig. 8). Under the above-described conditions, SMAD 1/5 phosphorylation was robustly induced in TM cells stimulated with GDF-15 for 24 hours (Figs. 8D, 8E). These results revealed activation of SMAD signaling pathway,s including the SMAD 2/3 and SMAD1/5 pathways, by GDF-15 in TM cells. Although the mechanism of action of GDF-15 at the receptor level is not completely understood, the activation of SMAD1/5 observed in TM cells suggests that GDF-15 may engage the activin receptor-like kinase 1 (ALK1). Reverse transcription-PCR analysis using ALK1 specific primers (Table) confirmed expression of this receptor protein in multiple human TM cell strains (Fig. 8F).

GDF-15–Induced Increases in ECM and ECM-Associated Proteins in TM Cells

Having confirmed that GDF-15 induces SMAD signaling, contractile activity, increased levels of αSMA, and fibronectin protein in TM cells, we further probed a possible role for GDF-

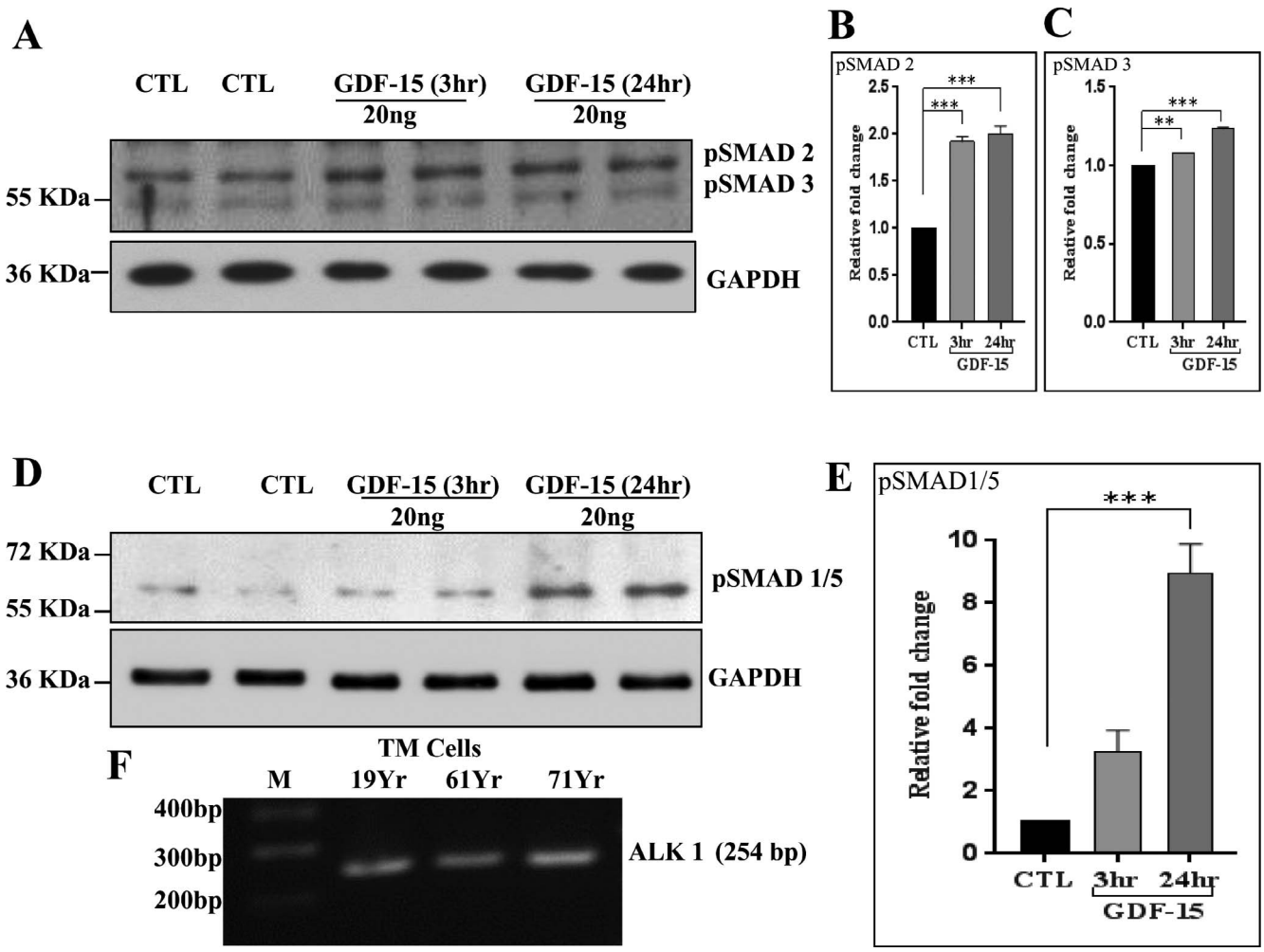

Figure 8. Growth differentiation factor-15 induced SMAD signaling in TM cells. Human TM cells were grown to confluence, serum-starved for 24 hours and treated with GDF-15 (20 ng/ml for 3 and 24 hours), followed by immunoblotting analysis of cell lysates to determine changes in SMAD phosphorylation. The GDF-15–treated TM cells showed a significant increase in the levels of phospho-SMAD 2/3 (**A**) and SMAD 1/5 (**D**) relative to control cells. Glyceraldehyde-3-phosphate dehydrogenase was used to normalize for loading. (**B**, **C**, **E**). Histograms depict the fold change in p-SMADs in GDF-15–treated cells compared to controls based on densitometric analysis. (**F**) Reverse transcription PCR–based detection of expression of ALK1 in human TM cells derived from different donors. Values are mean ± SEM. $n = 4$, $^{**}P \leq 0.01$; $^{***}P \leq 0.001$.

15 in ECM synthesis by TM cells. To this end, we used quantitative proteomics analysis to evaluate the effects of rGDF-15 on levels of ECM and ECM-associated proteins. As described in the Methods section, SDS and urea soluble fractions of ECM derived from human TM cells treated daily with rGDF-15 (20 ng/ml) for a period of 48 hours were subjected to mass spectrometry analysis. Based on data derived from two independent samples (using TM cells derived from 19- and 71-year-old donors), the levels of several different ECM and ECM-associated proteins were found increased in TM cells treated with rGDF-15, relative to untreated control cells. Supplementary Table S3 lists the proteins whose levels were increased by a minimum of 1.5-fold in GDF-15–treated TM cells. As expected, ECM-enriched fractions of TM cells contained not only several ECM proteins but also some cytoskeletal and cell adhesion proteins and proteases. Some notable ECM proteins whose levels were increased by rGDF-15 include elastin, versican, laminins, galectin-7, various collagen sub types, nidogen, fibulin-1, thombospondin, periostin, thrombospondin type1-domain containing protein, TIMP3, latent TGF-β binding proteins 1 and 2, plasminogen activation inhibitor-1and protein-glutamine γ-glutamyltransferase 2. These results revealed that GDF-15 can influence ECM production and organization in TM cells.

Discussion

Toward our long-term goal of understanding regulation of TM cell fibrogenic activity and the role of this cellular event in AH outflow dynamics and IOP, our recent efforts to perform comprehensive proteomics analysis of the ECM of TM cells revealed that GDF-15 is a common constituent of ECM secreted by the primary cultures of human TM cells.[9] This serendipitous observation motivated us to investigate the role of GDF-15 in TM cells, since it has been shown to be involved in various physiologic and pathologic processes, including fibrosis.[10–12,27,43] In this study, we reported not only that GDF-15 is expressed and secreted by TM cells, but also that expression of this growth factor is robustly induced by various external factors, including agents involved in glaucoma pathobiology. Our studies also revealed that GDF-15 regulates the contractile and adhesive properties of, and ECM production by TM cells. Taken together, this study suggested a potential role for GDF-15

in modulation of AH outflow and IOP in normal and glaucomatous eyes.

While it now is widely recognized that the autocrine and paracrine actions of factors secreted by the TM and SC cells influence their cellular characteristics with subsequent impact on AH outflow and IOP,[30,44–46] we lack comprehensive understanding of the identity of such factors. In this study, we showed that human TM cells express and secrete GDF-15. This multifunctional cytokine, which belongs to the TGF-β superfamily has a critical role in growth, differentiation and cell survival, and inflammation and apoptosis.[10,12,16,47] Initially identified in studies aimed at cloning genes of activated macrophages, GDF-15 was named MIC-1, since it suppresses the secretion of inflammatory cytokines, including TNF-α produced by macrophages.[14] Growth differentiation factor-15 levels are elevated under various pathologic conditions and this growth factor, therefore, is considered to be a prognostic marker for many diseases,[15–18] indicating that GDF-15 has a role in physiologic and pathologic processes similar to other members of the TGF-β family of cytokines.[48] Indeed, a common characteristic in glaucoma is the finding of increased levels of TGF-β2 in the AH.[49] This finding together with the demonstrated role of TGF-β in regulation of AH outflow and IOP, suggested the possibility that other cytokines of the TGF-β family, including GDF-15, also may have a role in homeostasis and dysregulation of AH outflow and IOP.[3,8,49]

Although the mature secreted form of GDF-15 is a homodimer with an expected molecular mass of 25 kDa, the latent secreted precursor form of GDF-15 has been reported to exhibit a varying molecular mass ranging from 30 to 40 kDa in different human specimens.[12] Growth differentiation factor-15 secreted from cultured human TM cells used in our study was found to exhibit a mass of approximately 36 kDa. Interestingly, GDF-15 in TM lysates and TM cell ECM fractions also exhibited the same molecular mass of approximately 36 kDa and was the predominant form recognized by a polyclonal antibody raised against full length recombinant human GDF-15 and by mass spectrometry analysis. It is possible that the precursor form of GDF-15, which is known to bind to ECM, may be the predominant form present in TM cells. Moreover, the precursor form is reported to be secreted faster than the mature form.[11]

Extensive literature exists regarding the ability of various inflammatory cytokines, tissue injury and other stressors to induce GDF-15 expression in target cells.[11,19,20,50,51] In TM cells, GDF-15 expression is robustly induced in response not only to TNF-α and IL-1β, but also to TGF-β2, dexamethasone, LPA, endothelin-1, and mechanical stretch as well. It is noteworthy that many of the extracellular factors tested in our studies for their effects on GDF-15 expression and secretion have been shown to regulate AH outflow and IOP, and that an increase in levels of several of these factors in the AH are correlated with increased IOP.[8,35,52,53] Therefore, it is plausible that GDF-15 participates in modulation of AH outflow resistance and IOP. This conclusion is supported further in part by the effects of *GDF-15* on gene expression in TM cells, particularly genes encoding proteins known to participate in fibrosis and connective tissue development/function and morphology and in cell death and survival.

Furthermore, the ability of rGDF-15 to induce increases in actin stress fibers and focal adhesions in association with increased phosphorylation of MLC and paxillin and levels of Hic-5 in TM cells demonstrates a role for this protein in regulation of cellular contractile and adhesive interactions which are recognized to influence AH outflow and IOP.[7,39,54] Interestingly, GDF-15 also has been shown to regulate the contractile and relaxation characteristics of the vascular endothelium by interacting with nitric oxide signaling.[29,55] Changes induced in cell morphology also have been found to alter the levels of GDF-15 protein.[56] Additionally, data from this study reveal that the GDF-15–induced increase in MLC phosphorylation is regulated in part via SMAD3 and Rho kinase–dependent intracellular signaling mechanisms in TM cells, similar to what is understood regarding the effects of TGF-β in TM and other cell types.[31,33,57,58] Thus, in future studies it would be interesting to explore the potential role of GDF-15 in integrin and Rho GTPase signaling in TM cells, since this factor has been shown to modulate cell adhesion and actin cytoskeletal organization via activation of focal adhesion kinase and Rho GTPase signaling in other cell types.[25] Moreover, in TM cells, GDF-15 stimulated an increase in the levels of αSMA, fibronectin, and several other ECM proteins, suggesting that it may have a physiologically relevant role in ECM homeostasis. Therefore, it is conceivable that increased levels of GDF-15 in the AH might lead to changes in cell plasticity and augment fibrogenic activity in TM cells, as is known to occur in other tissues.[43]

Intriguingly, most of the responses of TM cells to GDF-15 noted in this study are similar to those invoked by TGF-β2, including the effects of the latter on TM cell contractile activity, ECM synthesis, SMAD signaling and αSMA expression.[3,8] However, unlike TGF-β, which has been studied extensively in TM cells and is known to mediate its effects via engaging Type I and Type II membrane kinase receptors in various cell types,[59] the identity of receptor(s) and means of activation used by GDF-15 at the membrane receptor level are not clear.[12] Whether GDF-15 acts through the Type 1 and Type II TGF-β receptors or engages a unique ligand-specific receptor in TM cells must be explored. Recently, GDF-15 has been shown to interact with the ALK1 and to activate SMAD1 in epithelial cell type.[60] While ALK5 and TGFβRII are known to be involved in GDF-15–mediated biologic responses and activation of SMAD2/3 in different cell types,[26,29,61] activated ALK1 and TGFβRII also are known to induce expression of GDF-15 in endothelial cells.[62,63] In this study, we confirmed expression of ALK1 and activation of SMAD1/5, SMAD2, and SMAD3 by GDF-15 in human TM cells.

Additional support for our observations in this study on GDF-15 derives from a recent preliminary study from the Apte laboratory (Ban et al. *IOVS* 2016;57:ARVO E-Abstract 6020) at Washington University (St. Louis, MO, USA) reporting significantly increased levels of GDF-15 in the AH of glaucoma patients compared to control subjects, leading to the proposal that GDF-15 in AH may serve as a novel biomarker for glaucoma progression. On the other hand, it also is interesting to note that GDF-15 expression in naïve SC cells is increased in response to treatment with conditioned media derived from human SC cells subjected to selective laser trabeculoplasty (SLT) irradiation.[30] Although SLT treatment is known to lower IOP,[64] the functional significance of increased GDF-15 expression by SC cells subjected to this procedure is yet to be unraveled. The most puzzling aspect of GDF-15 biology is that it is known to participate in various cellular activities during early development and aging, and to elicit responses that are context- and tissue-specific. Growth differentiation factor-15 is not essential for early development with GDF-15 null mice reported to exhibit normal growth and fertility.[50] On the other hand, GDF-15 levels are elevated in numerous disease conditions suggesting a role for this factor in pathologic processes.[10,15,16,65] Moreover, increased levels of GDF-15 have been shown to induce inflammation, ER stress-induced apoptosis, mitochondrial dysfunction, senescence, and fibrosis in addition to have a role in the etiology of cancer, cardiac and several age-related chronic diseases.[15–18,23,25,43,60,66,67] Therefore, in future studies to investigate the role of GDF-15 in regulation of AH outflow and IOP, we plan to undertake

Investigative Ophthalmology & Visual Science

detailed assessment of the involvement of this cytokine in ocular hypertension and etiology of glaucoma.

Acknowledgments

The authors thank Harold Erickson from Duke University for providing the fibronectin polyclonal antibody.

Supported by NIH Grants R01EY018590 and P30-EY-005722.

Disclosure: A.**R. Muralidharan**, None; **R. Maddala**, None; **N.P. Skiba**, None; **P.V. Rao**, None

References

1. Kwon YH, Fingert JH, Kuehn MH, Alward WL. Primary open-angle glaucoma. *New Engl J Med*. 2009;360:1113–1124.
2. Gabelt BT, Kaufman PL. Changes in aqueous humor dynamics with age and glaucoma. *Prog Retin Eye Res*. 2005;24:612–637.
3. Tamm ER, Braunger BM, Fuchshofer R. Intraocular pressure and the mechanisms involved in resistance of the aqueous humor flow in the trabecular meshwork outflow pathways. *Prog Mol Biol Transl Sci*. 2015;134:301–314.
4. Wallace DM, Murphy-Ullrich JE, Downs JC, O'Brien CJ. The role of matricellular proteins in glaucoma. *Matrix Biol*. 2014; 37:174–182.
5. Freedman J, Iserovich P. Pro-inflammatory cytokines in glaucomatous aqueous and encysted Molteno implant blebs and their relationship to pressure. *Invest Ophthalmol Vis Sci*. 2013;54:4851–4855.
6. Wang N, Chintala SK, Fini ME, Schuman JS. Activation of a tissue-specific stress response in the aqueous outflow pathway of the eye defines the glaucoma disease phenotype. *Nat Med*. 2001;7:304–309.
7. Wiederholt M, Thieme H, Stumpff F. The regulation of trabecular meshwork and ciliary muscle contractility. *Prog Retin Eye Res*. 2000;19:271–295.
8. Wordinger RJ, Sharma T, Clark AF. The role of TGF-beta2 and bone morphogenetic proteins in the trabecular meshwork and glaucoma. *J Ocul Pharmacol Ther*. 2014;30:154–162.
9. Maddala R, Skiba NP, Rao PV. Vertebrate lonesome kinase regulated extracellular matrix protein phosphorylation, cell shape and adhesion in trabecular meshwork cells [published online ahead of print September 3, 2016]. *J Cell Physiology*. doi:10.1002/jcp.25582.
10. Unsicker K, Spittau B, Krieglstein K. The multiple facets of the TGF-beta family cytokine growth/differentiation factor-15/ macrophage inhibitory cytokine-1. *Cytokine Growth Factor Rev*. 2013;24:373–384.
11. Bauskin AR, Jiang L, Luo XW, Wu L, Brown DA, Breit SN. The TGF-beta superfamily cytokine MIC-1/GDF15: secretory mechanisms facilitate creation of latent stromal stores. *J Interferon Cytokine Res*. 2010;30:389–397.
12. Mimeault M, Batra SK. Divergent molecular mechanisms underlying the pleiotropic functions of macrophage inhibitory cytokine-1 in cancer. *J Cell Physiol*. 2010;224:626–635.
13. Paralkar VM, Vail AL, Grasser WA, et al. Cloning and characterization of a novel member of the transforming growth factor-beta/bone morphogenetic protein family. *J Biol Chem*. 1998;273:13760–13767.
14. Bootcov MR, Bauskin AR, Valenzuela SM, et al. MIC-1, a novel macrophage inhibitory cytokine, is a divergent member of the TGF-beta superfamily. *Proc Natl Acad Sci U S A*. 1997;94: 11514–11519.
15. Wang X, Baek SJ, Eling TE. The diverse roles of nonsteroidal anti-inflammatory drug activated gene (NAG-1/GDF15) in cancer. *Biochem Pharmacol*. 2013;85:597–606.
16. Breit SN, Johnen H, Cook AD, et al. The TGF-beta superfamily cytokine, MIC-1/GDF15: a pleotrophic cytokine with roles in inflammation cancer and metabolism. *Growth Factors*. 2011; 29:187–195.
17. Bauskin AR, Brown DA, Kuffner T, et al. Role of macrophage inhibitory cytokine-1 in tumorigenesis and diagnosis of cancer. *Cancer Res*. 2006;66:4983–4986.
18. Wiklund FE, Bennet AM, Magnusson PK, et al. Macrophage inhibitory cytokine-1 (MIC-1/GDF15): a new marker of all-cause mortality. *Aging Cell*. 2010;9:1057–1064.
19. Agarwal MK, Hastak K, Jackson MW, Breit SN, Stark GR, Agarwal ML. Macrophage inhibitory cytokine 1 mediates a p53-dependent protective arrest in S phase in response to starvation for DNA precursors. *Proc Natl Acad Sci U S A*. 2006; 103:16278–16283.
20. Zimmers TA, Jin X, Hsiao EC, McGrath SA, Esquela AF, Koniaris LG. Growth differentiation factor-15/macrophage inhibitory cytokine-1 induction after kidney and lung injury. *Shock*. 2005; 23:543–548.
21. Yang H, Filipovic Z, Brown D, Breit SN, Vassilev LT. Macrophage inhibitory cytokine-1: a novel biomarker for p53 pathway activation. *Mol Cancer Ther*. 2003;2:1023–1029.
22. Whitson RJ, Lucia MS, Lambert JR. Growth differentiation factor-15 (GDF-15) suppresses in vitro angiogenesis through a novel interaction with connective tissue growth factor (CCN2). *J Cell Biochem*. 2013;114:1424–1433.
23. Kempf T, Zarbock A, Widera C, et al. GDF-15 is an inhibitor of leukocyte integrin activation required for survival after myocardial infarction in mice. *Nat Med*. 2011;17:581–588.
24. Artz A, Butz S, Vestweber D. GDF-15 inhibits integrin activation and mouse neutrophil recruitment through the ALK-5/TGF-betaRII heterodimer. *Blood*. 2016;128:529–541.
25. Senapati S, Rachagani S, Chaudhary K, Johansson SL, Singh RK, Batra SK. Overexpression of macrophage inhibitory cytokine-1 induces metastasis of human prostate cancer cells through the FAK-RhoA signaling pathway. *Oncogene*. 2010;29:1293–1302.
26. Xu J, Kimball TR, Lorenz JN, et al. GDF15/MIC-1 functions as a protective and antihypertrophic factor released from the myocardium in association with SMAD protein activation. *Circ Res*. 2006;98:342–350.
27. Unal B, Alan S, Bassorgun CI, Karakas AA, Elpek GO, Ciftcioglu MA. The divergent roles of growth differentiation factor-15 (GDF-15) in benign and malignant skin pathologies. *Arch Dermatol Res*. 2015;307:551–557.
28. Lambrecht S, Smith V, De Wilde K, et al. Growth differentiation factor 15, a marker of lung involvement in systemic sclerosis, is involved in fibrosis development but is not indispensable for fibrosis development. *Arthritis Rheumatol*. 2014;66:418–427.
29. Heger J, Schiegnitz E, von Waldthausen D, Anwar MM, Piper HM, Euler G. Growth differentiation factor 15 acts anti-apoptotic and pro-hypertrophic in adult cardiomyocytes. *J Cell Physiol*. 2010;224:120–126.
30. Alvarado JA, Chau P, Wu J, Juster R, Shifera AS, Geske M. Profiling of cytokines secreted by conventional aqueous outflow pathway endothelial cells activated in vitro and ex vivo with laser irradiation. *Invest Ophthalmol Vis Sci*. 2015; 56:7100–7108.
31. Pattabiraman PP, Maddala R, Rao PV. Regulation of plasticity and fibrogenic activity of trabecular meshwork cells by Rho GTPase signaling. *J Cell Physiol*. 2014;229:927–942.
32. Pattabiraman PP, Rinkoski T, Poeschla E, Proia A, Challa P, Rao PV. RhoA GTPase-induced ocular hypertension in a rodent model is associated with increased fibrogenic activity in the trabecular meshwork. *Am J Pathol*. 2015;185:496–512.
33. Pattabiraman PP, Rao PV. Mechanistic basis of Rho GTPase-induced extracellular matrix synthesis in trabecular meshwork cells. *Am J Physiol Cell Physiol*. 2010;298:C749–C763.
34. Harvey A, Yen TY, Aizman I, Tate C, Case C. Proteomic analysis of the extracellular matrix produced by mesenchymal stromal

Investigative Ophthalmology & Visual Science

cells: implications for cell therapy mechanism. *PLoS One*. 2013;8:e79283.

35. Mettu PS, Deng PF, Misra UK, Gawdi G, Epstein DL, Rao PV. Role of lysophospholipid growth factors in the modulation of aqueous humor outflow facility. *Invest Ophthalmol Vis Sci*. 2004;45:2263–2271.
36. Shifera AS, Trivedi S, Chau P, Bonnemaison LH, Iguchi R, Alvarado JA. Constitutive secretion of chemokines by cultured human trabecular meshwork cells. *Exp Eye Res*. 2010;91:42–47.
37. Vittal V, Rose A, Gregory KE, Kelley MJ, Acott TS. Changes in gene expression by trabecular meshwork cells in response to mechanical stretching. *Invest Ophthalmol Vis Sci*. 2005;46:2857–2868.
38. Pattabiraman PP, Inoue T, Rao PV. Elevated intraocular pressure induces Rho GTPase mediated contractile signaling in the trabecular meshwork. *Exp Eye Res*. 2015;136:29–33.
39. Rao VP, Epstein DL. Rho GTPase/Rho kinase inhibition as a novel target for the treatment of glaucoma. *BioDrugs*. 2007;21:167–177.
40. Somlyo AP, Somlyo AV. Ca2+ sensitivity of smooth muscle and nonmuscle myosin II: modulated by G proteins, kinases and myosin phosphatase. *Physiol Rev*. 2003;83:1325–1358.
41. Thomas SM, Hagel M, Turner CE. Characterization of a focal adhesion protein, Hic-5, that shares extensive homology with paxillin. *J Cell Sci*. 1999;112:181–190.
42. Knipe RS, Tager AM, Liao JK. The Rho kinases: critical mediators of multiple profibrotic processes and rational targets for new therapies for pulmonary fibrosis. *Pharmacol Rev*. 2015;67:103–117.
43. Ishige T, Nishimura M, Satoh M, et al. Combined secretomics and transcriptomics revealed cancer-derived GDF15 is involved in diffuse-type gastric cancer progression and fibroblast activation. *Sci Rep*. 2016;6:21681.
44. Taurone S, Ripandelli G, Pacella E, et al. Potential regulatory molecules in the human trabecular meshwork of patients with glaucoma: immunohistochemical profile of a number of inflammatory cytokines. *Mol Med Rep*. 2015;11:1384–1390.
45. Parshley DE, Bradley JM, Samples JR, Van Buskirk EM, Acott TS. Early changes in matrix metalloproteinases and inhibitors after in vitro laser treatment to the trabecular meshwork. *Curr Eye Res*. 1995;14:537–544.
46. Bradley JM, Anderssohn AM, Colvis CM, et al. Mediation of laser trabeculoplasty-induced matrix metalloproteinase expression by IL-1beta and TNFalpha. *Invest Ophthalmol Vis Sci*. 2000;41:422–430.
47. Baek SJ, Kim KS, Nixon JB, Wilson LC, Eling TE. Cyclooxygenase inhibitors regulate the expression of a TGF-beta superfamily member that has proapoptotic and antitumorigenic activities. *Mol Pharmacol*. 2001;59:901–908.
48. Morikawa M, Derynck R, Miyazono K. TGF-beta and the TGF-beta family: context-dependent roles in cell and tissue physiology. *Cold Spring Harb Perspect Biol*. 2016;8.
49. Tripathi RC, Li J, Chan WF, Tripathi BJ. Aqueous humor in glaucomatous eyes contains an increased level of TGF-beta 2. *Exp Eye Res*. 1994;59:723–727.
50. Hsiao EC, Koniaris LG, Zimmers-Koniaris T, Sebald SM, Huynh TV, Lee SJ. Characterization of growth-differentiation factor 15, a transforming growth factor beta superfamily member induced following liver injury. *Mol Cell Biol*. 2000;20:3742–3751.
51. Kempf T, Eden M, Strelau J, et al. The transforming growth factor-beta superfamily member growth-differentiation factor-15 protects the heart from ischemia/reperfusion injury. *Circ Res*. 2006;98:351–360.
52. Gottanka J, Chan D, Eichhorn M, Lutjen-Drecoll E, Ethier CR. Effects of TGF-beta2 in perfused human eyes. *Invest Ophthalmol Vis Sci*. 2004;45:153–158.
53. Clark AF, Wilson K, de Kater AW, Allingham RR, McCartney MD. Dexamethasone-induced ocular hypertension in perfusion-cultured human eyes. *Invest Ophthalmol Vis Sci*. 1995;36:478–489.
54. Tian B, Geiger B, Epstein DL, Kaufman PL. Cytoskeletal involvement in the regulation of aqueous humor outflow. *Invest Ophthalmol Vis Sci*. 2000;41:619–623.
55. Mazagova M, Buikema H, Landheer SW, et al. Growth differentiation factor 15 impairs aortic contractile and relaxing function through altered caveolar signaling of the endothelium. *Am J Physiol Heart Circ Physiol*. 2013;304:H709–718.
56. Aw Yong KM, Zeng Y, Vindivich D, et al. Morphological effects on expression of growth differentiation factor 15 (GDF15), a marker of metastasis. *J Cell Physiol*. 2014;229:362–373.
57. Nakamura Y, Hirano S, Suzuki K, Seki K, Sagara T, Nishida T. Signaling mechanism of TGF-beta1-induced collagen contraction mediated by bovine trabecular meshwork cells. *Invest Ophthalmol Vis Sci*. 2002;43:3465–3472.
58. Meyer-ter-Vehn T, Sieprath S, Katzenberger B, Gebhardt S, Grehn F, Schlunck G. Contractility as a prerequisite for TGF-beta-induced myofibroblast transdifferentiation in human tenon fibroblasts. *Invest Ophthalmol Vis Sci*. 2006;47:4895–4904.
59. Heldin CH, Moustakas A. Signaling receptors for TGF-beta family members. *Cold Spring Harb Perspect Biol*. 2016;8.
60. Wu Q, Jiang D, Matsuda JL, Ternyak K, Zhang B, Chu HW. Cigarette Smoke Induces Human Airway Epithelial Senescence via GDF15 Production. *Am J Respir Cell Mol Biol*. 2016.
61. Min KW, Liggett JL, Silva G, et al. NAG-1/GDF15 accumulates in the nucleus and modulates transcriptional regulation of the Smad pathway. *Oncogene*. 2016;35:377–388.
62. Lee J, Fricke F, Warnken U, Schnolzer M, Kopitz J, Gebert J. Reconstitution of TGFBR2-mediated signaling causes upregulation of GDF-15 in HCT116 colorectal cancer cells. *PLoS One*. 2015;10:e0131506.
63. Lamouille S, Mallet C, Feige JJ, Bailly S. Activin receptor-like kinase 1 is implicated in the maturation phase of angiogenesis. *Blood*. 2002;100:4495–4501.
64. Damji KF, Shah KC, Rock WJ, Bains HS, Hodge WG. Selective laser trabeculoplasty v argon laser trabeculoplasty: a prospective randomised clinical trial. *Br J Ophthalmol*. 1999;83:718–722.
65. Wang X, Chrysovergis K, Kosak J, et al. hNAG-1 increases lifespan by regulating energy metabolism and insulin/IGF-1/mTOR signaling. *Aging*. 2014;6:690–704.
66. Fujita Y, Taniguchi Y, Shinkai S, Tanaka M, Ito M. Secreted growth differentiation factor 15 as a potential biomarker for mitochondrial dysfunctions in aging and age-related disorders. *Geriatr Gerontol Int*. 2016;16(suppl 1):17–29.
67. Park SH, Choi HJ, Yang H, et al. Two in-and-out modulation strategies for endoplasmic reticulum stress-linked gene expression of pro-apoptotic macrophage-inhibitory cytokine 1. *J Biol Chem*. 2012;287:19841–19855.

Investigative Ophthalmology & Visual Science